PHYSICAL REVIEW FLUIDS **6**, L112001 (2021)

Letter

Drops spreading on fluid surfaces: Transition from Laplace to Marangoni regime

Swaraj Deodhar, Sumesh P. Thampi,* and Madivala G. Basavaraj†
Polymer Engineering and Colloid Science Laboratory, Department of Chemical Engineering,
Indian Institute of Technology Madras, Chennai 600036, Tamilnadu, India

(Received 26 May 2021; accepted 20 October 2021; published 11 November 2021)

We show the occurrence of two distinguished classical regimes of wetting, namely, Laplace and solutal Marangoni, during the spreading of oil drops on a surfactant-laden aqueous phase in a single surfactant-oil-water system. The spreading kinetics is found to follow a power-law behavior not only in the Laplace and Marangoni regimes, but also in the transition regime. Our experimental findings are corroborated with the scaling laws. The results demonstrate that increasing the surfactant concentration across the critical micelle concentration is instrumental to obtain the Laplace to Marangoni transition. Moreover, this transition does not depend on surfactant chemistry; instead, it depends on the adsorption/desorption kinetics of surfactant molecules to/from the interfaces that are created or annihilated during drop spreading.

DOI: 10.1103/PhysRevFluids.6.L112001

The universality of the physics of wetting of one fluid on the surface of another is often captured by the power-law description of the spreading kinetics. Such descriptions are insightful in providing a mechanistic understanding of spreading encountered in oil spills [1], coating [2], pharmaceutical [3], petrochemical [4], and biological processes [5,6]. Although effects arising from gravity [7–9], inertia [10,11], activity [5], etc., may influence or even drive the spreading process, a balance of surface tension and viscous forces will invariably govern the spreading physics at a certain stage of spreading [1]. In this stage, the spreading can be driven by surface tension, referred to as Laplace spreading, or by a gradient in surface tension, referred to as Marangoni spreading. In the former regime, a drop (say of oil) of volume V will spread on a fluid-fluid interface (for example, a water-air interface), following a classical power law [1,12,13]—the radius of the spreading drop R increases with time t as

$$R \sim \left(\frac{\gamma_{oa} V^2 l}{\mu}\right)^{1/8} t^{1/8}, \tag{1}$$

where γ_{oa} is the oil-air interfacial tension, μ is the dynamic viscosity of the substrate liquid on which the oil drop spreads, and l is the characteristic height of the substrate liquid wherein the viscous dissipation predominantly occurs. On the other hand, in the Marangoni spreading regime, the power law takes the form [14,15]

$$R \sim \left(\frac{2S}{3\sqrt{\mu\rho}}\right)^{1/2} t^{3/4}, \tag{2}$$

---

[*] sumesh@iitm.ac.in
[†] basa@iitm.ac.in

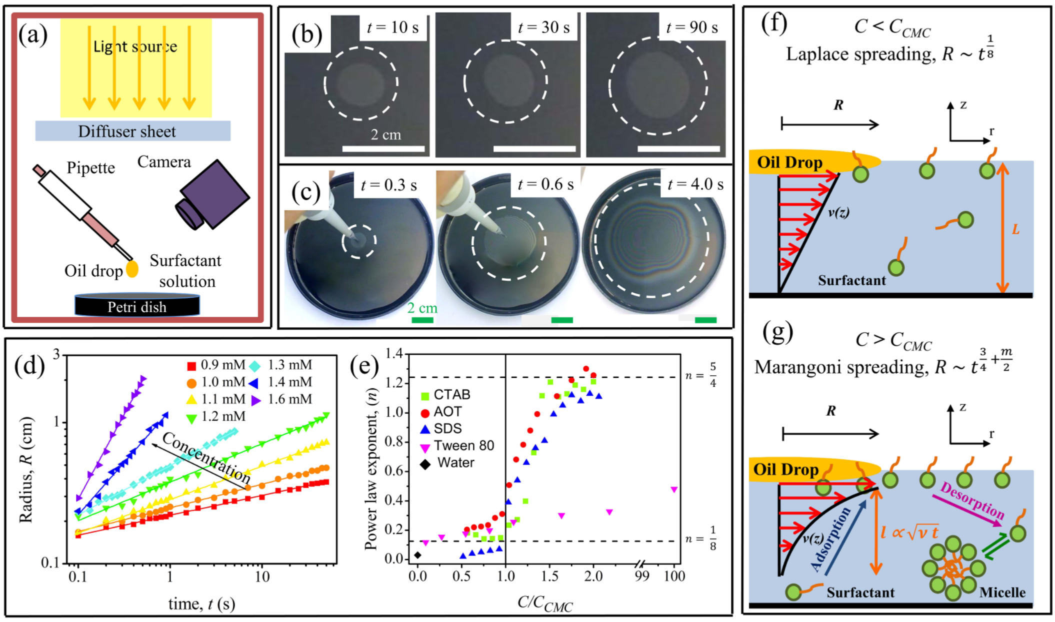

FIG. 1. (a) Schematic representation of the experimental setup used to study spreading of an oil drop on aqueous surfactant solutions. The top view of a 5 μl decane drop spreading on (b) 0.6 mM and (c) 2.0 mM aqueous CTAB solution as a function of time. The scale bar for each image in (b) and (c) represents 2 cm. A dashed circle is drawn to enable easy identification of the spreading drop from the background. (d) Spreading kinetics of oil drops on aqueous CTAB solutions of different concentrations. In all spreading experiments, the surfactant solution was taken in a Petri dish of diameter $d_p = 12.6$ cm, filled up to a height $L = 4$ mm, and allowed to equilibrate for 6 h before introducing a decane drop of volume, $V = 5$ μl. Schematic representation of the surfactant dynamics that occur during the spreading and the corresponding flow profile in (f) the Laplace regime ($C < C_{\mathrm{CMC}}$), which is characterized by the power-law scaling $R \sim t^{1/8}$ [Eq. (1)], and (g) the Marangoni regime ($C > C_{\mathrm{CMC}}$), which is characterized by the power-law scaling $R \sim t^{\frac{3}{4}+\frac{m}{2}}$ [Eq. (4)].

where S is the spreading coefficient [16] and ρ is the density of the substrate liquid. Although the drop spreading process in each of these regimes has been investigated individually [1,12–15], a connection between the two regimes or the transition from one regime to another still needs to be established.

In this Letter, we will establish the occurrence of the transition from Laplace to Marangoni spreading using model surfactant-oil-water systems. To this end, we consider the spreading of oil drops on surfactant-laden aqueous interfaces and vary the concentration of surfactant in the substrate liquid (aqueous phase) across the critical micelle concentration (CMC). The choice of model systems also provides a convenient way to tune the interfacial tension of the substrate liquid, which cannot be achieved in commonly studied systems, namely, spreading of surfactant-laden drops on pure liquids or solid surfaces. Further, the experimental study helps us test the fundamental theories of the spreading of drops on surfactant-laden liquids in the surfactant-lean and surfactant-rich regimes.

A schematic of the experimental setup used to image the spreading of oil drops dispensed on the surface of the surfactant-laden aqueous phase is shown in Fig. 1(a). In the experiments, a 5 μl decane drop (Bond number < 1) and a diverse set of commonly used surfactants of different chemistry, structure, and polarity, that is, cationic [cetyltrimethylammonium bromide (CTAB)], anionic [sodium dodecyl sulfate (SDS) single tailed, aerosol-OT (AOT) double tailed], and nonionic (Tween 80 and Triton X-100) surfactants are used. The concentration of surfactant C is varied over a large range across the critical micelle concentration C_{CMC} in all experiments (for more details, see Supplemental Material [17]).

Our experiments unambiguously reveal that irrespective of the surfactant, both the extent and rate of the spreading of oil drops on aqueous surfactant solutions are strikingly different when $C < C_{\mathrm{CMC}}$ and $C > C_{\mathrm{CMC}}$. To demonstrate this, we consider the spreading of oil drops on aqueous CTAB solutions ($C_{\mathrm{CMC}} = 1$ mM). Figures 1(b) and 1(c) show the top view of the oil drop at three different time instances during the course of spreading when the concentration of CTAB in the substrate liquid is 0.6 mM ($<C_{\mathrm{CMC}}$) and 2.0 mM ($>C_{\mathrm{CMC}}$), respectively. A comparison of the timescales and length scales shows that the extent and the rate of spreading are very different for $C < C_{\mathrm{CMC}}$ and $C > C_{\mathrm{CMC}}$. This difference is further quantified by following the temporal evolution of the radius of the oil drop at various CTAB concentrations as shown in Fig. 1(d). Clearly, the oil drop spreads at a slower rate and occupies a smaller interfacial area when $C < C_{\mathrm{CMC}}$ in comparison to the case of $C > C_{\mathrm{CMC}}$.

The increase in the extent of spreading of the oil drop with an increase in the concentration of the CTAB can easily be inferred by calculating the changes in the spreading coefficient, $S = \gamma'_{wa} - \gamma_{oa} - \gamma'_{wo}$, where, γ'_{wa} is the interfacial tension between the aqueous solution and air and γ'_{wo} is the interfacial tension between the aqueous solution and oil. Here, γ are the equilibrium interfacial tensions and the prime ($'$) in γ'_{wa} and γ'_{wo} indicates that interfacial tensions of pure liquids are modified due to the presence of surfactant in the substrate liquid. In our experiments, $S > 0$ and varies from $\approx$10.5 to $\approx$8.4 mN/m as the CTAB concentration varies from 0.6 to 2.0 mM (see Supplemental Material [17]). A higher S indicates a larger thermodynamic driving force and therefore oil drops spread to a larger extent when the concentration of CTAB in the aqueous solution is higher. However, a variation in S based on equilibrium interfacial tensions does not explain the change in the kinetics of spreading or the associated spreading mechanism. Therefore, we discuss below the physical picture associated with the complex spreading behavior.

Prior to dispensing the oil drop on the surface of the aqueous surfactant solution, the air-surfactant solution interface is in equilibrium and has a monolayer of surfactant at the interface. The introduction of the oil drop and the resulting spreading disrupts this equilibrium. The spreading of the oil compresses the surfactant monolayer leading to an increase in the concentration of surfactant molecules at the air-surfactant solution interface. Therefore, the air-aqueous solution interfacial tension decreases. Similarly, the concentration of surfactant molecules at the oil-surfactant solution interface decreases due to the expanding oil-water interfacial area, as a result of which the oil-surfactant solution interfacial tension increases as the spreading proceeds. Both these effects—the decrease in the interfacial tension of the air-surfactant solution interface and the increase in the interfacial tension of oil-surfactant solution interface—can potentially decrease the spreading coefficient. However, this change will be countered, if the surfactant molecules adsorb (or desorb) quickly to (from) the fluid-fluid interfaces. Moreover, the rate of adsorption of surfactant molecules to the oil-aqueous solution interface and the rate of desorption of surfactant molecules from the air-aqueous solution interface depends on the size and concentration of the surfactant molecules and their self-assembly in the aqueous phase. Our experiments reveal that the timescales associated with the adsorption of surfactant molecules are much larger than the timescales associated with the spreading of an oil lens. Therefore, the interfaces do not attain equilibrium during the timescale of spreading. Hence, the spreading coefficient does not remain constant during the process of spreading, an aspect which will be discussed later. To understand the dramatic change in the spreading kinetics that occurs with the change in the concentration of surfactant in the substrate liquid, we further analyze the temporal evolution of the radius of the spreading oil drop, $R(t)$, shown in Fig. 1(d). The spreading kinetics, irrespective of CTAB concentration, can be expressed as a power law, $R(t) \sim t^n$. The power-law exponent n increases systematically with an increase in CTAB concentration. A similar concentration-dependent power-law behavior is observed for all the surfactants considered (see Supplemental Material [17]).

The power-law exponents for the spreading oil drop dispensed on aqueous solutions containing cationic (CTAB), anionic (SDS, AOT), and nonionic (Tween 80) surfactants as a function of normalized surfactant concentration C/C_{CMC} are shown in Fig. 1(e). When $C/C_{\mathrm{CMC}} < 1$, the power-law exponent $n \approx \frac{1}{8}$ is relatively small and is insensitive to variation in the concentration of the surfactant. On the other hand, when $C/C_{\mathrm{CMC}} \approx 1$, n starts to increase drastically. Finally, n takes a value $n \approx \frac{5}{4}$ (except for Tween 80), which is independent of the surfactant concentration beyond $C/C_{\mathrm{CMC}} \approx 1.5$. We now demonstrate that this change in the value of n from the plateau corresponding to the lower surfactant concentration is due to a transition in the underlying mechanism of spreading.

When $C/C_{\mathrm{CMC}} < 1$, the power-law exponent $n \approx \frac{1}{8}$ corresponds to the Laplace spreading regime. A schematic of the drop spreading process in the low surfactant concentration regime is shown in Fig. 1(f). In this regime, the adsorption/desorption of surfactant to/from the interface has no significant role and the spreading occurs solely due to the gradient in the Laplace pressure. Since the Laplace pressure is proportional to the mean curvature of the oil drop, the gradient of Laplace pressure which scales as $\sim\gamma_{oa}\frac{h}{R^3}$ drives the spreading of the oil drop. Here, R and h respectively are the instantaneous radius and height of the spreading oil drop. As the pressure gradient acts over an area $\sim hR$, the stress acting on the interface between the aqueous solution and oil (the area of which scales as $\sim R^2$) is $\sim\gamma_{oa}\frac{h^2}{R^3}$. We note that this driving force is equivalent to the force due to the difference in the instantaneous and equilibrium contact angle of the drop [12] for the systems with a negative spreading coefficient. The balance between the viscous force, $\sim\mu\frac{dR/dt}{l}$, and the surface tension force, $\sim\gamma_{oa}(\frac{h^2}{R^3})$, gives the scaling law [Eq. (1)], which is derived by imposing the volume conservation condition $V \sim Rh^2$. The length scale $l = L$ is the thickness of the substrate liquid.

On the contrary, when $C/C_{\mathrm{CMC}} > 1$, the change in the interfacial tension due to the adsorption or desorption of the surfactant to or from the interface needs to be accounted for. The physical processes that occur during the spreading in this regime, referred to as the Marangoni spreading, are illustrated in Fig. 1(g). The driving force for spreading in this regime is the surface tension gradient. In line with earlier developments [14,15,18], the surface tension gradient is approximated as $S(t)/R$, where $S(t)$ is the instantaneous spreading coefficient given by $S(t) = \gamma'_{aw}(t) - \gamma'_{ow}(t) - \gamma_{oa}$. The surface tension gradient is balanced by the viscous forces $\mu\frac{dv}{dz}|_{z=0}$, where $\frac{dv}{dz}|_{z=0}$ is the velocity gradient evaluated at the oil-water interface ($z = 0$). As a result of the faster spreading of the oil drop, the momentum diffuses to a distance $l = \sqrt{\nu t} \ll L$, where ν is the kinematic viscosity of the substrate fluid. Approximating the velocity profile in this momentum boundary layer (of thickness δ) with an exponential function, the surface tension gradient-viscous force balance takes the form [15]

$$\frac{S(t)}{R} \sim \mu\frac{d}{dz}\left[\frac{dR}{dt}\exp{(z/\delta)}\right]\Bigg|_{z=0}. \tag{3}$$

Assuming the time-dependent spreading coefficient (as reflected from the dynamic surface tension measurements in the Supplemental Material [17] and data from the literature [19–24]) to follow a power law of the form $S \sim S_o(t/\tau)^m$, where S_o is the spreading coefficient corresponding to pristine interfaces (without surfactant) and τ is the characteristic time associated with the adsorption-desorption dynamics of the surfactant molecules to the interface [25], we obtain

$$R \sim \left(\frac{S_o}{(m+\frac{3}{2})\tau^m\sqrt{\mu\rho}}\right)^{1/2} t^{\frac{3}{4}+\frac{m}{2}}. \tag{4}$$

When $m = 0$, i.e., when the spreading coefficient is time independent, the classical power-law exponent corresponding to the Marangoni spreading regime [14,15], $n = 3/4$, is recovered.

Thus the spreading mechanism transitions from the Laplace to Marangoni regime as the concentration of surfactant in the substrate liquid is increased. A larger value of n in the Marangoni regime when compared to the Laplace regime indicates a faster spreading of the oil drop, consequently, a larger oil-water interfacial area is created at a given time instant. Thus in the Marangoni regime, the surfactant-free, nascent oil-water interface drives the transport of more surfactant molecules from the bulk to the interface when compared to the Laplace regime. The interplay of the dynamics of interface generation and surfactant adsorption/desorption to the interface results in a surfactant concentration-dependent exponent $\frac{3}{4}+\frac{m}{2}$. Interestingly, this nonequilibrium transition from Laplace to Marangoni spreading is continuous with the power-law exponent gradually changing from $n=\frac{1}{8}$ to $\frac{3}{4}+\frac{m}{2}$ as a function of concentration of the surfactant in the substrate liquid. The large value of power-law exponents observed in our experiments is reminiscent of the superspreading of surfactant-laden aqueous drops on hydrophobic solid surfaces [26]. Interestingly, the spreading exponents observed in superspreading exhibit a large variation in the vicinity of $C \approx C_{\mathrm{CMC}}$, followed by a plateau [27,28] similar to the data shown in Fig. 1(e).

Since there exists a plateau $n \approx \frac{5}{4}$ beyond $C/C_{\mathrm{CMC}} \approx 1.5$, we can back calculate the value of m from the experimental data shown in Fig. 1(e) to be $m=1$. Thus the time-dependent spreading coefficient follows $S \sim t$. A deviation from this general picture is exhibited by the bulkier surfactant molecules, Tween 80 (and Triton X-100, as discussed later). The experimentally determined value of m for all other surfactant molecules in this regime is in accordance with the theoretical considerations reported in Wodlei *et al.* [25]. It may be possible to advance the Laplace to Marangoni spreading transition to occur at $C < C_{\mathrm{CMC}}$ instead of occurring at $C = C_{\mathrm{CMC}}$, which appears to be the case in previous works [18,25], where the dispensed drop dissolves in the substrate liquid, thereby inducing surface tension gradients even when $C < C_{\mathrm{CMC}}$.

To distill the essential physics associated with drop spreading in a manner discussed in this Letter, it is of utmost important to achieve a separation of length scales along and perpendicular to the direction of the spreading drop. The scaling in the Laplace spreading regime is realized by ensuring $h \ll L \ll R$ which corresponds to (i) the viscous dissipation in the drop being negligible compared to that in the substrate liquid ($h\mu \ll L\mu_{\mathrm{oil}}$ [13]), (ii) the flows are primarily one dimensional (along the spreading direction), and (iii) the thickness of the substrate liquid layer in which viscous dissipation occurs remains constant ($l = L$) throughout the spreading process (~10–100 s). Similarly, in our experiments, the scaling in the Marangoni regime ($C > C_{\mathrm{CMC}}$) is realized by ensuring that the boundary layer thickness beneath the spreading drop $\sqrt{\nu t} \ll L$, since the spreading occurs over a timescale of ~0.1–1 s which corresponds to a boundary layer thickness of ≈0.1–1.0 mm.

Therefore, a careful choice of parameters—substrate liquid height $L = 4$ mm, Petri dish diameter $d_p = 12.6$ cm, substrate liquid equilibration time in the Petri dish prior to spreading experiments $t_{\mathrm{eq}} = 6$ h, volume of the oil drop $V = 5\ \mu$l, and varying the concentration of surfactant in the substrate liquid across CMC—enabled the identification of both Laplace and Marangoni spreading regimes using the power-law exponents ($n=\frac{1}{8}$ for $C < C_{\mathrm{CMC}}$ and $n=\frac{5}{4}$ for $C > C_{\mathrm{CMC}}$) and hence unearthed the transition from the Laplace to Marangoni spreading regime in a single set of experiments for a given surfactant-water-oil system as presented in Figs. 1(b)–1(e). The transition from the Laplace to Marangoni regime is a robust phenomenon and can be observed over a large range of parameter space as is evident from the data for more than 100 spreading experiments presented in Figs. 2(a) and 2(b). The power-law exponent n is relatively insensitive to all the parameters, except when $L = 2$ mm, the lowest substrate liquid height considered in this work. This difference is most likely due to the backflow of the substrate liquid [29].

Other examples where deviations from the expected values of the exponents ($n=\frac{1}{8}$ and $n=\frac{5}{4}$) occur is when the substrate liquid contains bulkier surfactant molecules. Due to their lower molecular diffusivity, diffusive transport processes in the substrate liquid, i.e., the kinetics of adsorption/desorption, are severely affected. Hence the change in the spreading coefficient during the spreading process may not follow $S \sim t$, the scaling described earlier, and bulkier surfactant molecules will show deviations from the spreading kinetics discussed above. The case of Tween 80 ($M_w = 1310$ g/mol) is presented in Fig. 1(e). For Triton X-100 ($M_w = 647$ g/mol), another bulkier surfactant molecule, the spreading cannot be described by a single power-law exponent, as shown in Fig. 2(c). Instead, the spreading occurs in two stages, consistent with previous observations [30], as discussed in detail in the Supplemental Material [17,31,32]. The first stage occurs when $t < 20$ s, and in this stage, the spreading kinetics above and below CMC are identical, i.e., a power-law behavior with $n \approx \frac{1}{8}$ is observed independent of the concentration of Triton X-100. On the other

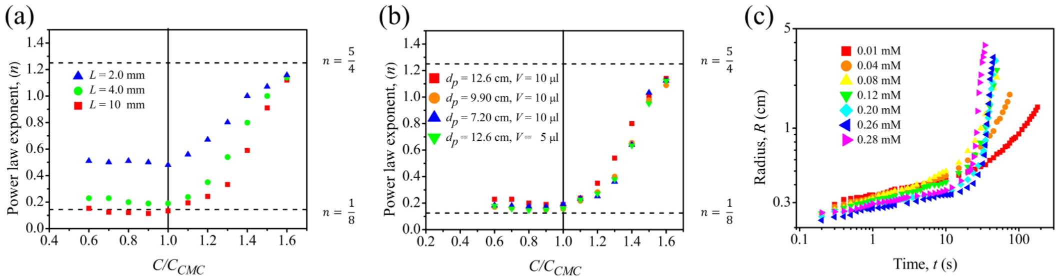

FIG. 2. Effect of (a) substrate liquid height (L) and (b) Petri dish diameter (d_p) and drop volume (V) on the power-law exponent (n) for the spreading of a decane drop on an aqueous CTAB solution of concentrations varying across CMC. (c) Spreading kinetics of decane drops on aqueous Triton X-100 solutions when the concentration of the surfactant is varied across CMC ($C_{\mathrm{CMC}} = 0.25$ mM). Other experimental conditions are the same as those described in the caption of Fig. 1.

hand, the spreading kinetics in the second stage, which occurs when $t > 20$ s, no longer follows a power law. But, in this stage, the rate of spreading increases significantly for concentrations above CMC compared to lower concentrations, yet again indicating a transition in the spreading mechanism.

To summarize, in this Letter, we illustrated the transition from a surface tension-driven slow spreading Laplace regime, to a surface tension gradient-driven fast spreading Marangoni regime. Our analysis provides a framework for achieving this spreading transition, the crucial parameter being the availability of surfactant molecules for the interface-bulk exchange. Such an exchange enhances the spreading kinetics in the Marangoni regime with a larger power-law exponent $n = 5/4$. The fundamental insights of spreading kinetics presented in our study is expected to be of relevance in several fields, such as environmental, personal care, medical applications, and other research areas such as active matter [5,6,18,33–35].

We wish to acknowledge Pankaj Rohilla (Chemical Engineering, Texas Tech University) for initiating this work and Professor M. Manivannan (Applied Mechanics, IIT Madras) for discussion.

[1] D. P. Hoult, Oil spreading on the sea, Annu. Rev. Fluid Mech. **4**, 341 (1972).

[2] J. A. Moriarty, L. W. Schwartz, and E. O. Tuck, Unsteady spreading of thin liquid films with small surface tension, Phys. Fluids A **3**, 733 (1991).

[3] K. Koch, B. Dew, T. E. Corcoran, T. M. Przybycien, R. D. Tilton, and S. Garoff, Surface tension gradient driven spreading on aqueous mucin solutions: A possible route to enhanced pulmonary drug delivery, Mol. Pharm. **8**, 387 (2011).

[4] D. O. Shah, *Improved Oil Recovery by Surfactant and Polymer Flooding* (Elsevier, Amsterdam, 2012).

[5] M. A. Fardin, O. M. Rossier, P. Rangamani, P. D. Avigan, N. C. Gauthier, W. Vonnegut, A. Mathur, J. Hone, R. Iyengar, and M. P. Sheetz, Cell spreading as a hydrodynamic process, Soft Matter **6**, 4788 (2010).

[6] J.-F. Joanny and S. Ramaswamy, A drop of active matter, J. Fluid Mech. **705**, 46 (2012).

[7] C. Yang, A. Burrous, J. Xie, H. Shaikh, A. Elike-Avion, L. Rojas Rodriguez, A. Ramachandran, W. Choi, and A. D. Mazzeo, High-gravity spreading of liquid puddles on wetting flexible substrates, Appl. Phys. Lett. **108**, 074102 (2016).

[8] N. D. DiPietro, C. Huh, and R. G. Cox, The hydrodynamics of the spreading of one liquid on the surface of another, J. Fluid Mech. **84**, 529 (1978).

[9] R. Chebbi, Viscous-gravity spreading of time-varying liquid drop volumes on solid surfaces, J. Colloid Interface Sci. **300**, 688 (2006).

[10] M. R. Rahman, H. N. Mullagura, B. Kattemalalawadi, and P. R. Waghmare, Droplet spreading on liquid–fluid interface, Colloids Surf., A **553**, 143 (2018).

[11] M. Motaghian, R. Shirsavar, M. Erfanifam, M. Sabouhi, E. van der Linden, H. A. Stone, D. Bonn, and M. Habibi, Rapid spreading of a droplet on a thin soap film, Langmuir **35**, 14855 (2019).

[12] J. F. Joanny, Wetting of a liquid substrate, PCH, PhysicoChem. Hydrodyn. **9**, 183 (1987).

[13] J. G. E. M. Fraaije and A. M. Cazabat, Dynamics of spreading on a liquid substrate, J. Colloid Interface Sci. **133**, 452 (1989).

[14] S. Berg, Marangoni-driven spreading along liquid-liquid interfaces, Phys. Fluids **21**, 032105 (2009).

[15] V. Bergeron and D. Langevin, Monolayer Spreading of Polydimethylsiloxane Oil on Surfactant Solutions, Phys. Rev. Lett. **76**, 3152 (1996).

[16] P.-G. De Gennes, F. Brochard-Wyart, and D. Quéré, *Capillarity and Wetting Phenomena: Drops, Bubbles, Pearls, Waves* (Springer, Berlin, 2013).

[17] See Supplemental Material at http://link.aps.org/supplemental/10.1103/PhysRevFluids.6.L112001 for details of materials and experimental methods, and additional data concerning spreading kinetics and dynamic surface tension.

[18] H. Kim, K. Muller, O. Shardt, S. Afkhami, and H. A. Stone, Solutal Marangoni flows of miscible liquids drive transport without surface contamination, Nat. Phys. **13**, 1105 (2017).

[19] H. Vatanparast, F. Shahabi, A. Bahramian, A. Javadi, and R. Miller, The role of electrostatic repulsion on increasing surface activity of anionic surfactants in the presence of hydrophilic silica nanoparticles, Sci. Rep. **8**, 7251 (2018).

[20] A. Bak and W. Podgórska, Interfacial and surface tensions of toluene/water and air/water systems with nonionic surfactants Tween 20 and Tween 80, Colloids Surf., A **504**, 414 (2016).

[21] J. K. Ferri and K. J. Stebe, Which surfactants reduce surface tension faster? A scaling argument for diffusion-controlled adsorption, Adv. Colloid Interface Sci. **85**, 61 (2000).

[22] N. R. Biswal, N. Rangera, and J. K. Singh, Effect of different surfactants on the interfacial behavior of the n-hexane–water system in the presence of silica nanoparticles, J. Phys. Chem. B **120**, 7265 (2016).

[23] V. B. Fainerman, S. V. Lylyk, E. V. Aksenenko, L. Liggieri, A. V. Makievski, J. T. Petkov, J. Yorke, and R. Miller, Adsorption layer characteristics of triton surfactants: Part 2. Dynamic surface tension and adsorption, Colloids Surf., A **334**, 8 (2009).

[24] R. Miller, E. V. Aksenenko, and V. B. Fainerman, Dynamic interfacial tension of surfactant solutions, Adv. Colloid Interface Sci. **247**, 115 (2017).

[25] F. Wodlei, J. Sebilleau, J. Magnaudet, and V. Pimienta, Marangoni-driven flower-like patterning of an evaporating drop spreading on a liquid substrate, Nat. Commun. **9**, 820 (2018).

[26] R. M. Hill, Superspreading, Curr. Opin. Colloid Interface Sci. **3**, 247 (1998).

[27] S. Rafaï, D. Sarker, V. Bergeron, J. Meunier, and D. Bonn, Superspreading: Aqueous surfactant drops spreading on hydrophobic surfaces, Langmuir **18**, 10486 (2002).

[28] S. Rafaı and D. Bonn, Spreading of non-Newtonian fluids and surfactant solutions on solid surfaces, Physica A **358**, 58 (2005).

[29] R. N. O'Brien, A. I. Feher, and J. Leja, Interferometric and hydrodynamic flow profiles produced in water by a spreading monolayer, J. Colloid Interface Sci. **51**, 366 (1975).

[30] Y. Cheng, X. Ye, and H. R. Ma, Solidlike spreading of a liquid/liquid system, Appl. Phys. Lett. **89**, 181906 (2006).

[31] P.-M. Gassin, G. Martin-Gassin, D. Meyer, J.-F. Dufrêche, and O. Diat, Kinetics of Triton-X100 transfer across the water/dodecane interface: Analysis of the interfacial tension variation, J. Phys. Chem. C **116**, 13152 (2012).

[32] P.-M. Gassin, R. Champory, G. Martin-Gassin, J.-F. Dufrêche, and O. Diat, Surfactant transfer across a water/oil interface: A diffusion/kinetics model for the interfacial tension evolution, Colloids Surf., A **436**, 1103 (2013).

[33] C. C. Maass, C. Krüger, S. Herminghaus, and C. Bahr, Swimming droplets, Annu. Rev. Condens. Matter Phys. **7**, 171 (2016).

[34] D. Bonn, J. Eggers, J. Indekeu, J. Meunier, and E. Rolley, Wetting and spreading, Rev. Mod. Phys. **81**, 739 (2009).

[35] A. L. Yarin, Drop impact dynamics: Splashing, spreading, receding, bouncing …, Annu. Rev. Fluid Mech. **38**, 159 (2006).